Chemistry Research Journal, 2023, 8(2):32-41

Available online www.chemrj.org

Research Article

ISSN: 2455-8990
CODEN(USA): CRJHA5

Spectroscopic Studies, Thermal Analysis and Molecular Docking of Amikacin Metal Complexes

Gehan S. Elasala, Soad S. Fyala, Alaa E. Ali*

Chemistry Department, Faculty of Science, Damanhour, Damanhour University, Egypt

Abstract Synthesis and spectrothermal characterization of new amikacin complexes with metal [Cr(III), Mn(II), Fe(III), Co(II), Ni(II), Cu(II), Zn(II), Cd(II) and Hg(II)] salts are reported. The structural chemistry of these complexes is achieved via elemental analysis, spectral (UV, visible, and IR), thermal (DTA and TGA) as well as magnetic susceptibility. New tetrahedral complexes of amikacin acts as a bidentate ligand. Amikacin complexes show higher activity than amikacin for some strains. The geometry of the complexes is converted from Oh to Td during their thermal decomposition. The decomposition mechanisms are suggested and the thermodynamic parameters for the thermal decomposition steps are evaluated. molecular docking simulation outcomes that predicted a strong binding of amikacin to the breast cancer protein (3s7s).

Keywords coordination chemistry, Thermal analysis, Decomposition mechanisms, amikacin, Complexes, Biological activity, molecular docking

1. Introduction

Amikacin is an antibiotic medication used for a number of bacterial infections Figure (1). [1] This includes joint infections, intra-abdominal infections, meningitis, pneumonia, sepsis, and urinary tract infections. [2] It is also used for the treatment of multidrug-resistant tuberculosis. [3] Amikacin works by blocking the function of the bacteria's 30S ribosomal subunit, making it unable to produce proteins. Amikacin was patented in 1971, and came into commercial use in 1976. It is on the World Health Organization's List of Essential Medicines. It is derived from kanamycin. [4] Thermal analysis plays an important role in investigating the structure and the properties of metal complexes. Alaa E. Ali *et al.* reported the complexing properties and thermal behavior of some biologically active compounds [5–14]. The main purpose of this work is to study the complexing properties and thermal behavior of Amikacin ligand and its metal complexes. Amikacin can form a five-membered ring with metal ion during complexations which gives high stability to the formed complexes. The thermal decomposition mechanism is explained and the thermodynamic parameters are evaluated.

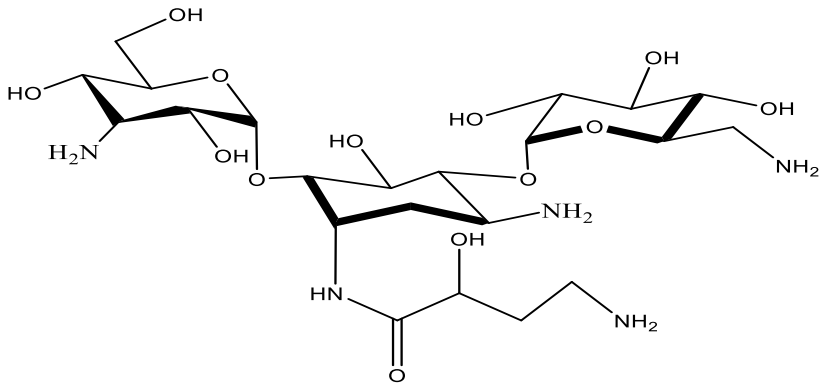

Figure 1: Structure of amikacin Ligand

2. Experimental

Some metal [Cr(III), Mn(II), Fe(III), Co(II), Ni(II), Cu(II), Zn(II), Cd(II) and Hg(II)] chlorides are complexed with amikacin ligand by a similar procedure. The metal chloride and ligand are dissolved in adequate volumes of ethanol separately. The molar amount of the metal chloride salt is mixed with the calculated amount of the ligand using mole ratio (M:L) viz. 1:1., the reaction mixture is refluxed for about 2 hours then left over-night, where the precipitated complexes were separated by filtration, then washed several times with a mixture of EtOH–H_2O and dried in a vacuum desiccator over anhydrous $CaCl_2$. The analytical results are given in Table 1. Elemental analyses of the synthesized complexes were done by the usual methods [15]. The metal contents were determined by using atomic absorption spectrophotometer (model 6650 Shimadzu) and complexmetrically with standard EDTA solution using the appropriate indicator as reported [16]. The chloride content of the complexes is determined by applying the familiar Volhard method [15]. The proposed structures of synthesized metal complexes were illustrated in Figure (2). The KBr disc IR spectra of the ligand and its complexes were measured over the frequency range 400–4000 cm^{-1} using Perkin-Elmer Spectrophotometer. The UV–Vis spectra of the solid complexes were measured in Nujol mull spectra [17]. Molar magnetic susceptibilities, corrected for diamagnetism using Pascal's constants were determined at room temperature (298 K) using Faraday's method. The instrument was calibrated with $Hg[Co(SCN)_4]$. DTA and TGA analyses are carried out using a Shimadzu DTA/TGA-50. The rate of heating was 10 °C/min and the atmospheric nitrogen rate flow was 20 ml min^{-1}. The biological screening of amikacin and their metal complexes were examined against 5 microorganisms representing different microbial categories, {two Gram-positive (Staphylococcus Aureas ATCC6538P and Bacillus subtilis ATCC19659), two Gram negative (Escherischia coli ATCC8739 strain and Pseudomonas aeruginosa ATCC9027) and candida albicans as a fungi .A molecular docking study was conducted by the Molecular Operating Environmental module (MOE 2015.10). The 3D structure of the selected protein 3s7s was adopted from the protein data bank. As docking initial steps, the protein structure was set up by removing water molecules and adding hydrogen atoms. Also, a site finder was used for the ligand-binding site prediction. Evaluation of the best binding pose between the investigated ligands and the receptor protein was based on the H-bond length and the scoring energy of the simulated docked complex.

Table 1: Elemental analysis, m.p, formula, stoichiometries and colour of (Amikacin) complexes

Complexes	**Colour**	**Calculated/(Found)%**				
		C	**H**	**N**	**M**	**Cl**
[Cr(Amikacin)$(Cl)_2$]	violet	37.35	5.98	9.90	7.35	10.02
		(37.39)	(5.96)	(9.91)	(7.31)	(10.03)
[Mn (Amikacin) (Cl)(H_2O)]	Yellow	38.13	6.40	10.11	7.93	5.12
		(38.14)	(6.41)	(10.13)	(7.49)	(5.13)
	Dark	37.15	5.95	9.85	7.85	9.97
[Fe(Amikacin)Cl_2]	brown	(37.16)	(5.97)	(9.88)	(7.86)	(9.98)

[Co(Amikacin)(Cl)(H_2O)]	Orange	37.91	6.36	10.05	8.46	5.09
		(37.93)	(6.38)	(10.07)	(8.48)	(5.11)
[Ni(Amikacin)(Cl)(H_2O)]	Green	37.92	6.37	10.05	8.42	5.09
		(37.93)	(6.38)	(10.09)	(8.44)	(5.08)
[Cu(Amikacin)(Cl)(H_2O)]	Brown	37.66	6.32	9.98	9.06	5.05
		(37.69)	(6.36)	(9.96)	(9.08)	(5.03)
[Zn(Amikacin)(Cl)(H_2O)]	white	37.56	6.30	6.96	9.29	5.04
		(37.55)	(6.33)	(6.98)	(9.31)	(5.14)
[Cd (Amikacin)(Cl)(H_2O)]	white	35.21	5.91	9.33	14.98	4.72
		(35.22)	(5.93)	(9.32)	(14.91)	(4.71)
[Hg(Amikacin)(Cl)(H_2O)]	white	31.51	5.29	8.35	23.92	4.23
		(31.52)	(5.33)	(8.33)	(29.94)	(4.25)

3. Results and Discussion

3.1 IR spectra of amikacin and its metal complexes

Amikacin possess a number of lone pair rich sites, and amine substituted lactone ring ,which gives ability to form complexes . The broad bands at 3350 –3362 cm^{-1} in the systems could be assigned to ν_{O-H} involved in hydrogen bond, due to the presence of coordinated water molecules in all prepared complexes It seems from the elemental analysis of the complexes and thermal analysis that all complexes contain water molecules in their structures. This is evident by ν_{OH}, Table (2). However, coordinated water in these complexes is indicated by the appearance of metal-oxygen bands attributable to rocking modes at 407 – 412 cm^{-1} region[18] .The complexation is confirmed through IR bands of free amikacin and the metal complexes where the spectra have two very strong absorption peaks at 1751 cm^{-1} of lactone and 1653 cm^{-1} due to ketonic carbonyl groups . The absorption peaks of 1000 cm^{-1} is due to the ethers while the peak of 1249 cm^{-1} is due to amine functional group. The CH_2 bending is due to peaks between 1345 and 1465 cm^{-1} ,while alkane stretching peaks appeared among 2800-2880 cm^{-1}. Coordinated water appeared as bands between 3353 and 3652 cm^{-1} with peak maxima at 3652 cm^{-1}. In metal complexes of amikacin , some very prominent peak shifting has been observed along with change in intensities of several important peaks indicating amikacin has undergo complexation with metals as shown in Table (72 In [Mn (Amikacin) (Cl)(H_2O)]] complex as an example, the aliphatic amine of amikacin with the peak of 1249 cm^{-1} was shifted to 1165cm^{-1}.The same results were observed in amikacin with all prepared metal complexes. In the light of these observations, it can be fairly concluded that the N ($CH3)_2$ group of desosamine and hydroxyl group, have been utilized in the complex formation. In the far IR spectra, the bonding of oxygen is provided by the presence of bands at 407cm^{-1} (M-O).

Table 2: Fundamental infrared bands (cm^{-1}) of Amikacin and its metal complexes

Compound	N_{OH} of H_2O	ν(lactone)	ν(C=O)	ν (amine)	ν (CH_2)	ν_{M-N}	ν_{M-O}
Amikacin	-	1752	1653	1249	1345	-	-
[Cr(Amikacin)$(Cl)_2$] H_2O	3652	1754	1651	1165	1461	477	407
[Mn (Amikacin) (Cl)(H_2O)]	3593	1753	1653	1174	1462	496	406
[Fe(Amikacin)Cl_2].H_2O	3591	1754	1655	1185	1463	476	405
[Co(Amikacin)(Cl)(H_2O)]	3592	1755	1654	1166	1463	489	405
[Ni(Amikacin)(Cl)(H_2O)]	3520	1754	1653	1166	1463	489	406
[Cu(Amikacin)(Cl)(H_2O)]	3528	1754	1654	1167	1463	475	407
[Zn(Amikacin)(Cl)(H_2O)]	3596	1755	1654	1168	1463	473	409
[Cd (Amikacin)(Cl)(H_2O)]	3598	1753	1655	1164	1463	474	411
[Hg(Amikacin)(Cl)(H_2O)]	3352	1772	1653	1169	1465	474	412

3.2 Electronic spectral and magnetic studies

The electronic absorption spectra for the green chromium-complex [Cr(Amikacin)$(Cl)_2$] showed three bands at 278, 427, 461 nm Table (3) and Figure (2) due to $^4A_{2g}\rightarrow{}^4T_{2g}$ (F), $^4A_{2g}\rightarrow{}^4T_{1g}$(F) and $^4A_{2g}\rightarrow{}^4T_{1g}$(p) of tetrahedral structure and the μ_{eff} value which equals, 4.82B.M, while [Mn (Amikacin) (Cl)(H_2O)] gave bands at 262 and 446, while the last bands in each complex are due to $^6A_{1g}\rightarrow{}^4T_{1g}$. Its room temperature μ_{eff} value of 5.8 B.M, typified the existence of Td configuration. However the brown electronic absorption spectra of [Fe(Amikacin)Cl_2] gave bands at 259, 442, 630 nm the last bands is due to $^6A_{1g}\rightarrow{}^4T_{1g}$. Its room temperature μ_{eff} value of 4.8 B.M, typified the existence of Td configuration. While the electronic absorption spectra of [Co(Amikacin)(Cl)(H_2O)], gave bands at 250, 437 nm the last one due to $^4A_2\rightarrow{}^4T_1$(p) with magnetic moment value equal to 4.3 B.M typified the existence of the complex in Td geometry. while the electronic absorption spectra of [Ni(Amikacin)(Cl)(H_2O)] showed two bands at 260 ,427 nm where the last one due to $^3T_1$(F)$\rightarrow{}^3T_1$(p) transitions of tetrahedral geometry with μ_{eff} value(3.1) B.M. while [Cu(Amikacin)(Cl)(H_2O)] showed bands at 260, 355 nm ,which are assigned to the transition $^2T_2 \rightarrow {}^2E_g$, to suggest tetrahedral structure geometry with room temperature μ_{eff} value is 1.74 B.M. Zinc, cadmium and mercury complexes of both drug ligands didn't gave visible spectra. All of them were found to be diamagnetic in nature and assumed to be of tetrahedral geometry like the rest transition metal ions under investigation.

Table 3: Nujol mull electronic absorption spectra λ_{max} (nm), room temperature effective magnetic moment values (μ_{eff}, 298°K) and geometries of Amikacin metal complexes

Complex	λ_{max} (nm)	μ_{eff}	Geomety
[Cr(Amikacin)$(Cl)_2$]	278, 427, 461	4.8	Td
[Mn (Amikacin) (Cl)(H_2O)]	262 446	5.8	Td
[Fe(Amikacin)Cl_2]	259, 442,630	4.8	Td
[Co(Amikacin)(Cl)(H_2O)]	250, 437	4.3	Td
[Ni(Amikacin)(Cl)(H_2O)]	260, 427	3.1	Td
[Cu(Amikacin)(Cl)(H_2O)]	262, 455	1,74	Td
[Zn(Amikacin)(Cl)(H_2O)]	212	Diamagnetic	Td
[Cd (Amikacin)(Cl)(H_2O)]	230	Diamagnetic	Td
[Hg(Amikacin)(Cl)(H_2O)]	215	Diamagnetic	Td

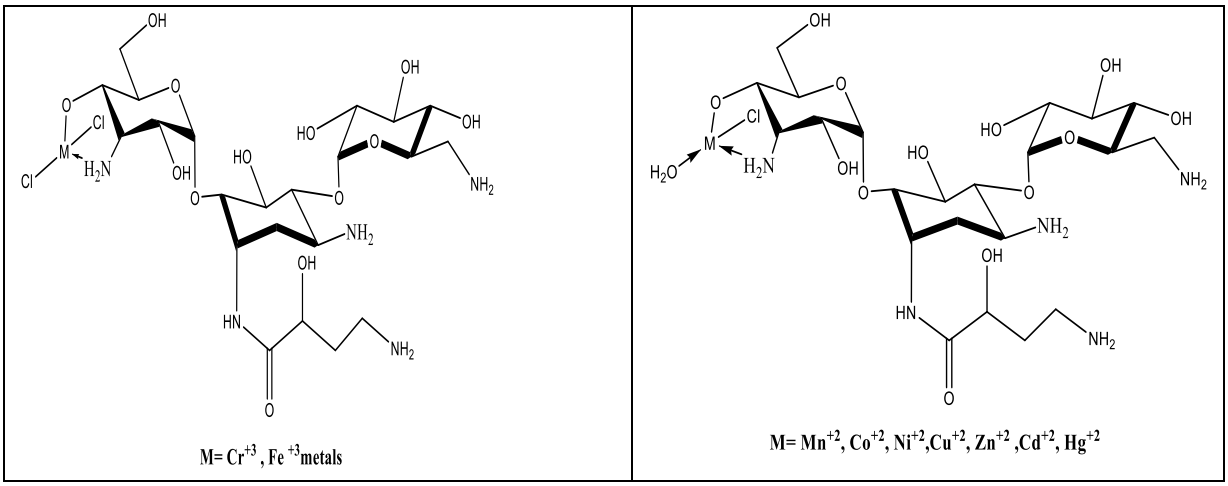

Figure 2: Proposed structures of amikacin complexes

3.3 Electron Spin Resonance of Copper Complex

The room temperature polycrystalline X-band ESR spectral pattern of [Cu(Amikacin)(Cl)(H_2O)] complex, Figure(3) is isotropic nature with gx= 2.15 and value of A= 130 .The presence of ESR signals at g<4 may assign the spin-spin interaction between the Cu atoms show the diametric nature of complex.

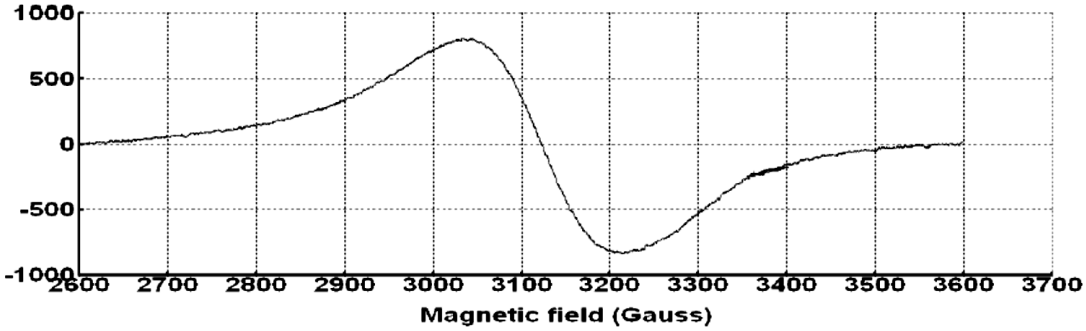

Figure 3: [Cu(Amikacin)(Cl)(H_2O)]

3.4 Thermal analysis investigations

the thermal DTA sheet of **the free ligand " Amikacin "**, Figures (4) and Table (4), showed two peaks at.160 and 347, °C with activation energies 85.96 and 95.42kJ/mole, respectively. The orders of reactions were 0.7 and 2.03, , respectively. The first peak is endothermic while the second is exothermic type, scheme (1):

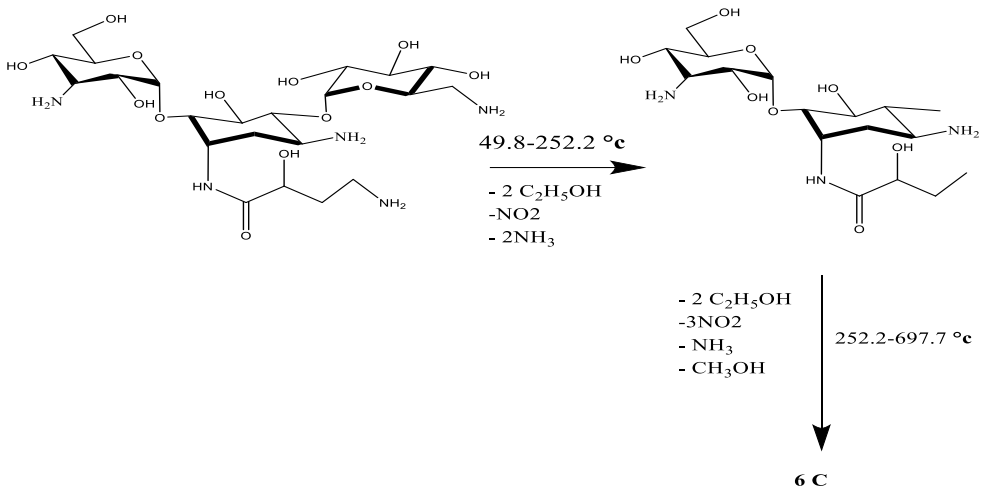

Scheme (1): thermolysis of Amikacin

For an example the [Cr(Amikacin)$(Cl)_2$] complex, Figures (4) and Table (4), showed two well defined peaks at 109.1, and 541.6 °C from the DTA data with activation energies of 36.03 and 86.65 kJ/mole, their reaction orders were 1.56, 0.45, respectively. All peaks are exothermic except the first peak is endothermic type. Scheme (2):

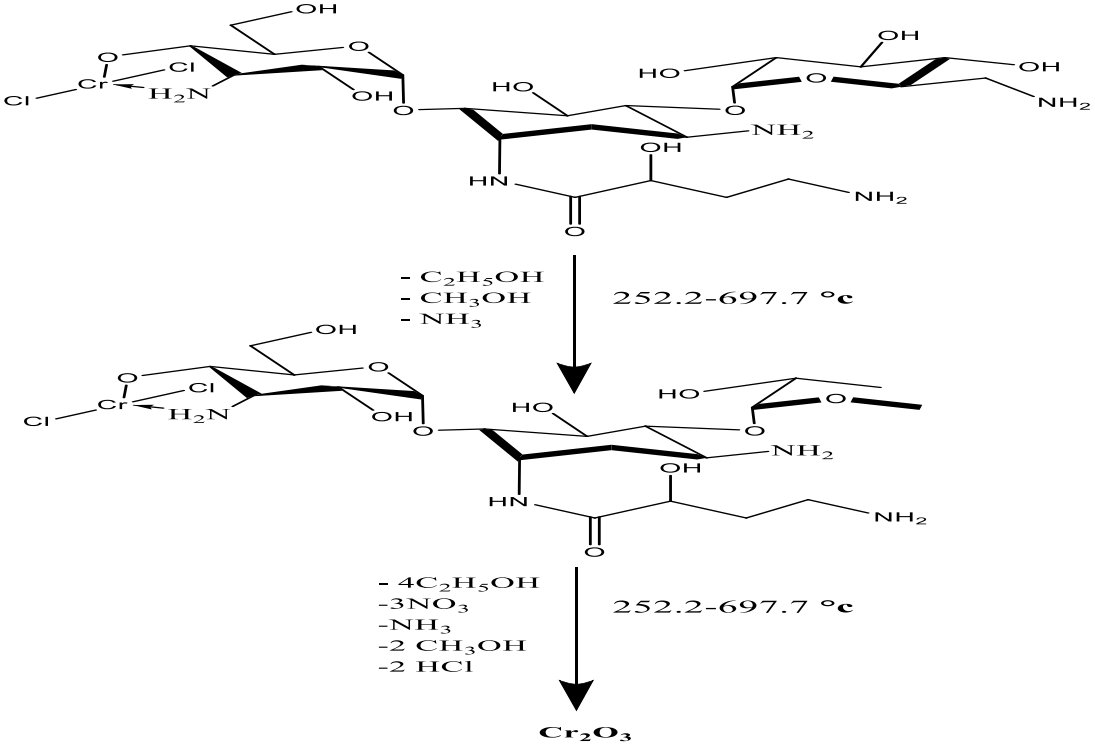

Scheme (2): thermolysis of [Cr(Amikacin)$(Cl)_2$]

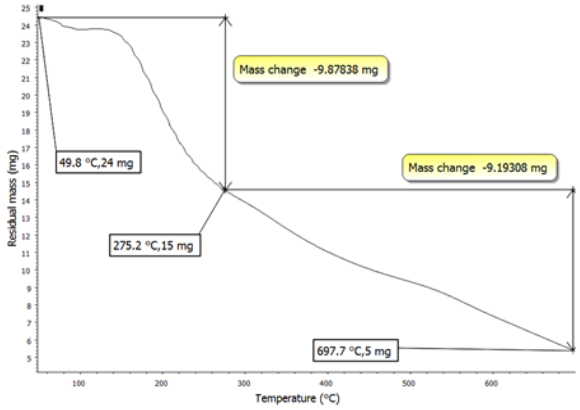

TGA of Amikacin

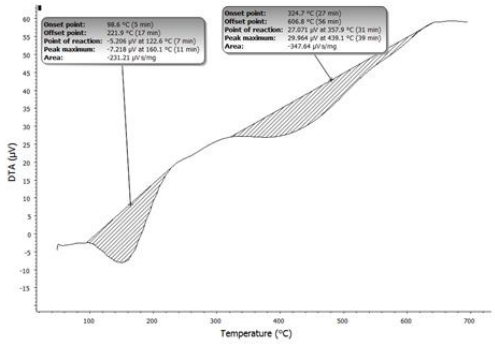

DTA of Amikacin

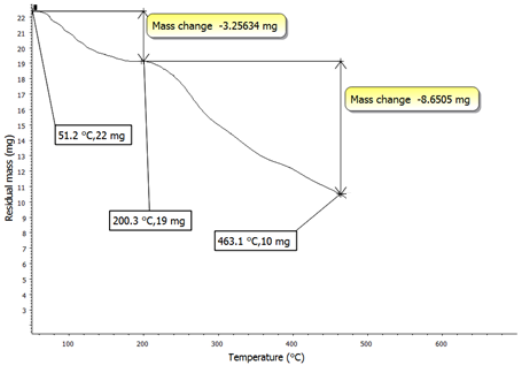

TGA of [Cr (Amikacin)$(Cl)_2$]

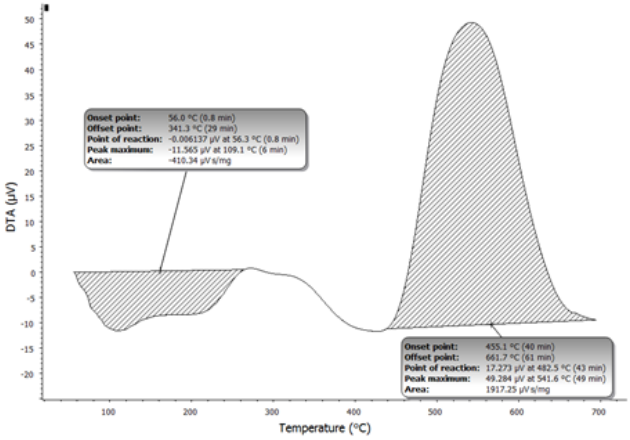

DTA of [Cr (Amikacin)$(Cl)_2$]

Figure 4: TGA and DTA of Amikacin and its chroumium complex

Table 4: DTA analysis of Amikacin and its metal complexes

Complex	**Type**	**Tm (°K)**	**E_a kJ mol^{-1}**	**n**	**α_m**	**$\Delta S^{\#}$ kJ K^{-1} mol^{-1}**	**$\Delta H^{\#}$ kJ mol^{-1}**	**Z S^{-1}**	**Temp. (°C) TGA**	**Wt. Loss %** Calc	Found	**Assignment**
Amikacin	Endo	160	85.96	0.70	0.69	-0.27	-29.56	0.096	49.8-275.2°C	37.51	37.51	Loss of 2 C_2H_5OH, NO_2 and 2 NH_3
	Exo	347	95.42	2.03	0.49	-0.28	-44.92	0.071	275.2-697°C	79.16	79.18	Loss of 2 C_2H_5OH, NO_2, CH_3OH and NH_3
[Cr (Amikacin)$(Cl)_2$]	Endo	109.1	36.03	1.56	0.54	-0.28	-39.28	0.031	51.2-200.3°C	13.63	13.62	Loss of NH_3, C_2H_5OH and CH_3OH
	Exo	541.6	86.65	0.45	0.76	-0.29	-120.3	0.025	200.3-463°C	54.54	54.56	Loss of NH_3, 4 C_2H_5OH, NO_2 and 2 CH_3OH.

[Mn (Amikacin) (Cl)(H_2O)]	Endo	99.8	37.56	1.23	0.59	-0.28	-30.60	0.041	58-313.2°C	20.07	20.08	Dehydration of H_2O and loss of NH_3, C_2H_5OH and CH_3OH
	Endo	480	131.8	1.78	0.52	-0.29	-111.14	0.041	313.2-697°C	46.06	46.08	Loss of NO_2, $2C_2H_5OH$ and CH_3OH

3.5 Biological activity

Most of the metal complexes have higher activity[19-20]than the free ligands such increased activity of the metal chelates could be explained on the bases of overtonės concept and chelation theory. In this study, 5 microorganisms representing different microbial categories, {two Gram-positive (*Staphylococcus Aureas* ATCC6538P *and* Bacillus subtilis ATCC19659), two Gram negative (Escherischia coli ATCC8739 strain and Pseudomonas aeruginosa ATCC9027) bacteria were used Table (5). The study included, ligand **amikacin** and 2 complexes of different metal ions (Zn and Cu)}. Four different broadly antibiotics (**Ciprofloxacin** *and* **Clotrimazole**) are used in this study as references. [Cu(Amikacin)(Cl)(H_2O)] and [Zn(Amikacin)(Cl)(H_2O)] complex showed activity in the same range of amikacin for Escherischia coli, Staphyllococcus aureus *and* Bacillus subtilis.

Table 5: The antifungal activity of the free ligands and its complexes against some reference strains expressed in absolute activity (AU)

Biological compounds	***Candida albicans***		***Escherischia coli***		***Pseudomonas aeruginosa***		***Staphyllococcus aureus***		***Bacillus subtilis***	
		Cpd.		**Cpd.**		**Cpd.**		**Cpd.**		**Cpd.**
[Cu(Amikacin)(Cl)(H_2O)]	8	8	8	12	8	8	8	12	8	11
[Zn(Amikacin)(Cl)(H_2O)]	8	8	8	12	8	8	8	12	8	11
chloramphenicol	8	12	8	12	8	8	8	12	8	11
Amikacin	8	8	8	12	8	8	8	12	8	11
Ciprofloxacin	9	30	9	30	9	30	9	30	-	-
Clotrimazole	-	-	-	-	-	-	-	-	10	17

3.6 Molecular docking.

Docking investigation is an essential step preceding the in vitro study of any proposed biologically active compound. This approach elucidates the ligand-receptor site and type of interactions. It also gives an estimation of the distance between the ligand and the receptor inside the interaction grid. The scoring energy of each pose simulated by the docking calculations reflects the degree of inhibition effect of the corresponding

ligand. In the present study, the selected protein 3s7s represents the crystal structure of the human placentalany proposed biologically active compound. This approach elucidates the ligand-receptor site and type of interactions. It also givesan estimation of the distance between the ligand and the receptor inside the interaction grid. The scoring energy of each pose simulated by the docking calculations reflects the degree of inhibition effect of the corresponding ligand. In the present study, the selected protein 3s7s represents the crystal structure of the human placental aromatase enzyme that catalyzes the synthesis of estrogen hormone and contributes to estrogen-dependent breast cancer. All ligands possess an appreciable extent of interactions with the receptor protein based on the scoring energy . The result show the abibilty of ligand to inhibt 3s7s protien Figure (5,6) .

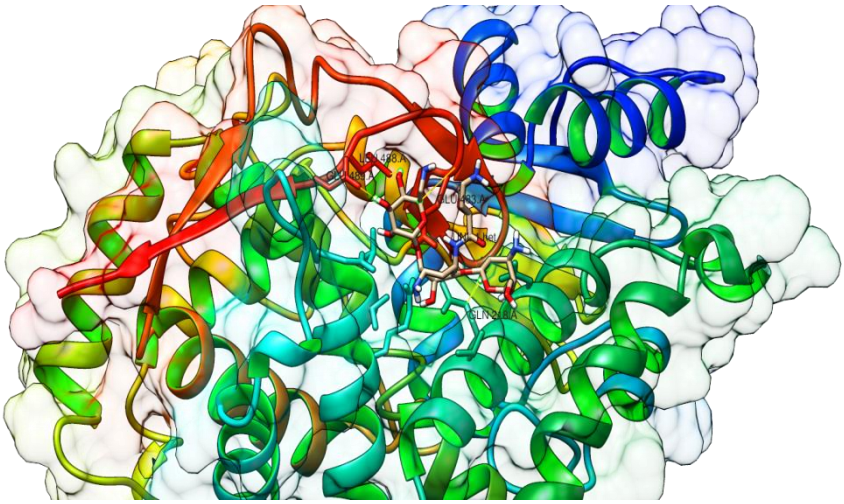

Figure 5: Virtual Molecular docking of amikacin with 3s7s protein

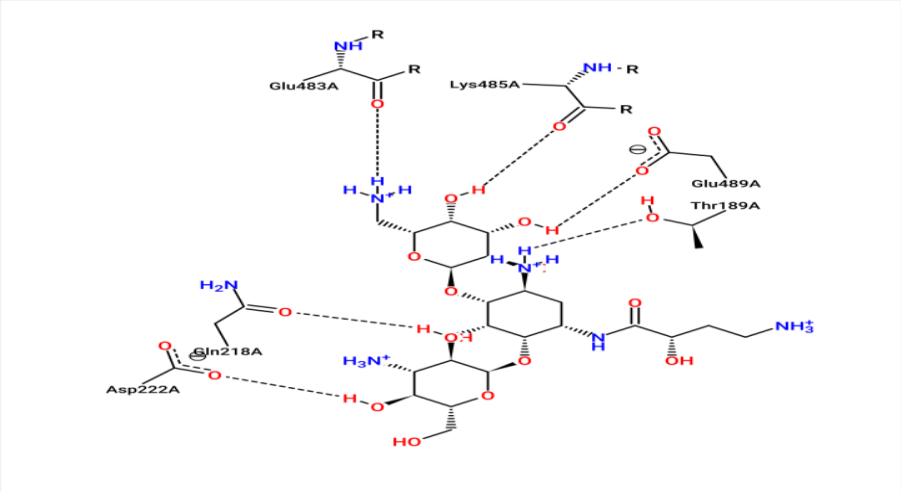

Figure 6: 2D structure of Molecular docking of amikacin with 3s7s protein

References

[1]. Bukvi´c Kraja˘ci´c, M.; Peri´c, M.; Smith, K.S.; Ivezi´c Schönfeld, Z.; Žiher, D.; Fajdeti´c, A.; Kujundži´c, N.; Schönfeld, W.; Landek, G.; Padovan, J.,J. Med. Chem. 2011, 54, 3595–3605.

[2]. The American Society of Health-System Pharmacists. Archived from the original on 20 December 2016.

[3]. Stuart MC, Kouimtzi M, Hill SR (eds.). WHO Model Formulary. World Health Organization. **2008**, 137-139.

[4]. World Health Organization model list of essential medicines: 21st list **2019**. Geneva.

[5]. Kolkaila S.A. , Ali A.E. , Elasala G.S. ,, Int J Cur Res Rev., 13, 23, 53-59, (2021).

[6]. Masoud M.S., Ali A.E., Elasala G.S., kolkaila S.A., Spectrochim. Acta., 193, (2018) 458-466.

[7]. Masoud M.S., Ali A.E., Elasala G.S., kolkaila S.A., J. Chem. Pharm. Res. 9, (2017) 171-179.

[8]. Ali A. E., Elasala G. S., Mohamed E. A., kolkaila S.A., heliyon, 5(11), (2019).

[9]. Ali A. E., Elasala G. S., Mohamed E. A., kolkaila S.A., , J. materials today proceeding https://doi.org/10.1016/j.matpr.2020.12.403 (2021).

[10]. Masoud M.S., Ali A.E., Elasala G.S., sakr S.F, kolkaila S.A.,Structural, J. Chem. Pharm. Res. 12, (2020) 42-52.

[11]. Masoud M.S., Ali A.E., Elasala G.S., sakr S.F, kolkaila S.A., J. Chem. Pharm. Res. 12, (2020) 29-41.

[12]. Ali Alaa E, Elasala Gehan S, Atta Rana M and Kolkaila Sherif A, Chemistry Research Journal, 7(2) (2022), 90-99.

[13]. Kolkaila Sherif A., Ali Alaa E., Beltagy Doha, Elasala Gehan S., Journal of Drug Design and Research, 2(5) (2018), 1071-1079**.**

[14]. Elmelegy Essam and Kolkaila Sherif A. Ali Alaa E., Mustafa Ahmed A., Eledkawy Abdelmonem Mohamed A, Ahmed M, Alnaggar Gehan A, Journal of Environmental Treatment Techniques, 10(2) (2022), 164-169.

[15]. Thorburn Burns D (1978) Vogel's textbook of quantitative inorganic analysis, including elementary instrumental analysis 4th edn: revised by J. Bassett, R.C. Denney, G.H. Jeffery and J. Mendham, Longman, London and New York, 106, pp 925, DOI: 10.1016/S0003-2670(01)83721.

[16]. Lee R.H, Griswold E, Kleinberg J (1964) Studies on the stepwise controlled decomposition of 2, 2'-bipyridine complexes of cobalt (II) and nickel (II) chlorides, Inorg. Chem., 3, 1278-1283. http://doi.org/10.1021/ic50019a018.

[17]. Lee R.H, Griswold E, Kleinberg J (1964) Studies on the stepwise controlled decomposition of 2, 2'-bipyridine complexes of cobalt (II) and nickel (II) chlorides, Inorg. Chem., 3, 1278-1283. http://doi.org/10.1021/ic50019a018.

[18]. Howlader M. B. H, M. S. Islam and Karim M. R, J. Chem, 39 A, **2000**; 407.

[19]. Hammud H. H, Holman K. T, Masoud M. S, El-Faham A. and Beidas H, Inorg. Chem. Acta, **2009**; 362 (10), 3526.

[20]. Masoud M. S, Hagagg S. S, Ali A.E and Nasr N. M, J. Mol. Struct., **2012;** 1014, 1.